State-Dependent Inactivation of the Kv3 Potassium Channel

Shimon Marom and Irwin B. Levitan

Graduate Department of Biochemistry and Center for Complex Systems, Brandeis University, Waltham, Massachussetts 02254 USA

ABSTRACT Inactivation of Kv3 (Kv1.3) delayed rectifier potassium channels was studied in the Xenopus oocyte expression system. These channels inactivate slowly during a long depolarizing pulse. In addition, inactivation accumulates in response to a series of short depolarizing pulses (cumulative inactivation), although no significant inactivation occurs within each short pulse. The extent of cumulative inactivation does not depend on the voltage during the depolarizing pulse, but it does vary in a biphasic manner as a function of the interpulse duration. Furthermore, the rate of cumulative inactivation is influenced by changing the rate of deactivation. These data are consistent with a model in which Kv3 channel inactivation is a state-dependent and voltage-independent process. Macroscopic and single channel experiments indicate that inactivation can occur from a closed (silent) state before channel opening. That is, channels need not open to inactivate. The transition that leads to the inactivated state from the silent state is, in fact, severalfold faster then the observed inactivation of current during long depolarizing pulses. Long pulse-induced inactivation appears to be slow, because its rate is limited by the probability that channels are in the open state, rather than in the silent state from which they can inactivate. External potassium and external calcium ions alter the rates of cumulative and long pulse-induced inactivation, suggesting that antagonistic potassium and calcium binding steps are involved in the normal gating of the channel.

INTRODUCTION

Despite extensive study, the mechanism of so-called slow or C-type inactivation in delayed-rectifier potassium channels remains enigmatic. Inactivation has been described as a voltage-dependent process in some preparations (for review see Hille, 1992), voltage and state-dependent (Aldrich, 1981), or exclusively state-dependent (Cahalan et al., 1985; DeCoursey, 1990) in others. It is not clear that all delayed rectifier channels inactivate via a common mechanism. Moreover, in several cases it has been shown that a single process cannot account for the inactivation in a particular channel (Grissmer and Cahalan, 1989; Koren et al., 1990). In the past few years, several cloned delayed rectifier channels have become available. Mutation studies, aimed at locating a slow inactivation "gate", suggest that no specific structure can account entirely for the process (Hoshi et al., 1991; Busch et al., 1991). Kv3 (Kv1.3) is a delayed rectifier channel, cloned from rat brain (Stühmer et al., 1989; Swanson et al., 1990) and found also in T lymphocytes (Grissmer et al., 1990; Douglass et al., 1990). Inactivation of Kv3 is particularly intriguing because it has characteristics that make it significant from a physiological point of view: it demonstrates cumulative inactivation (Cahalan et al., 1985; Marom et al., 1993), it is modulated by the intracellular en-

vironment (Cahalan et al., 1985; Marom et al., 1993; Honore et al., 1992), and it is affected by extracellular potassium (Grissmer and Cahalan, 1989; Pardo et al., 1992) and calcium (Grissmer and Cahalan, 1989) ions. The purpose of the present study is to examine the mechanism of inactivation of Kv3 channels, to provide a biophysical framework for structure-function studies. Our data are consistent with a model in which inactivation is a state-dependent but voltage-independent process that is accessible at a fast rate from a pre-opened nonconducting (silent) state. The probability of the channel being in this silent state limits the rate of inactivation; hence, the apparent slow rate of inactivation during a long pulse. Macroscopic and single channel data suggest that cumulative inactivation is not a separate phenomenon, but also involves entry of the channel into the inactivated state from the silent state. Finally, we suggest a mechanism for the effect of external potassium and calcium ions on Kv3 inactivation kinetics.

MATERIALS AND METHODS

Biophysical Journal

RESULTS

Mechanism of cumulative inactivation

Upon depolarization, within a physiological range of pulse durations (<15 ms), the Kv3 channel demonstrates inactivation that is not related directly to the *duration* of the depolarizing pulse, but rather depends on the *frequency* at which pulses are delivered to the membrane (Marom et al., 1993). This phenomenon has been termed cumulative inactivation (Aldrich, 1981) and is demonstrated qualitatively in Fig. 1. In Fig. 1 *a*, current responses to a train of 20 successive 5-ms pulses to the same voltage are superimposed. Note the very slow deactivation rate during the interpulse period; as will be shown later, this plays a key role in the induction of cumulative inactivation. As shown by Aldrich (1981), DeCoursey (1990), and Lee and Deutsch (1990), cumulative inactivation is dependent on the frequency of pulsing in a biphasic manner (Fig. 1, *b* and *c*). More than 30 s of interpulse hyperpolarization at −80 mV are required for the channels to "forget" completely the effect of previous stimulations. Shorter interpulse intervals (<30 s and >600 ms), result in cumulative inactivation (Fig. 1 *b*); however, at the very shortest range of interpulse intervals (<600 ms), inactivation

becomes less profound as the intervals are decreased (Fig. 1 *c*). The result of Fig. 1 *c* is very close qualitatively and quantitatively to what Lee and Deutsch (1990) have shown for the human T-lymphocyte Kv channel. The rate of cumulative inactivation is independent of membrane potential in the range where the channel is fully activated (Fig. 1 *d*). The observations summarized in Fig. 1 clearly are not consistent with a classic voltage-dependent, state-independent inactivation model.

Which is the state (or states) that provides access to the inactivated state? We have reported previously (Marom et al., 1993), based on similarities in recovery rates, tetraethylammonium (TEA) sensitivity and modulatory effects, that the state into which channels are driven during cumulative inactivation is identical to the state into which channels are driven during long depolarizing pulses. Therefore, any scheme that accounts for cumulative inactivation should also account for long pulse-induced inactivation without the addition of states. Under this constraint, two general types of model are possible (see schemes below): a coupled model, in which channels must open (O^*) before entering the inactivated state (I), was suggested by DeCoursey (1990) to describe inactivation of alveolar epithelial potassium
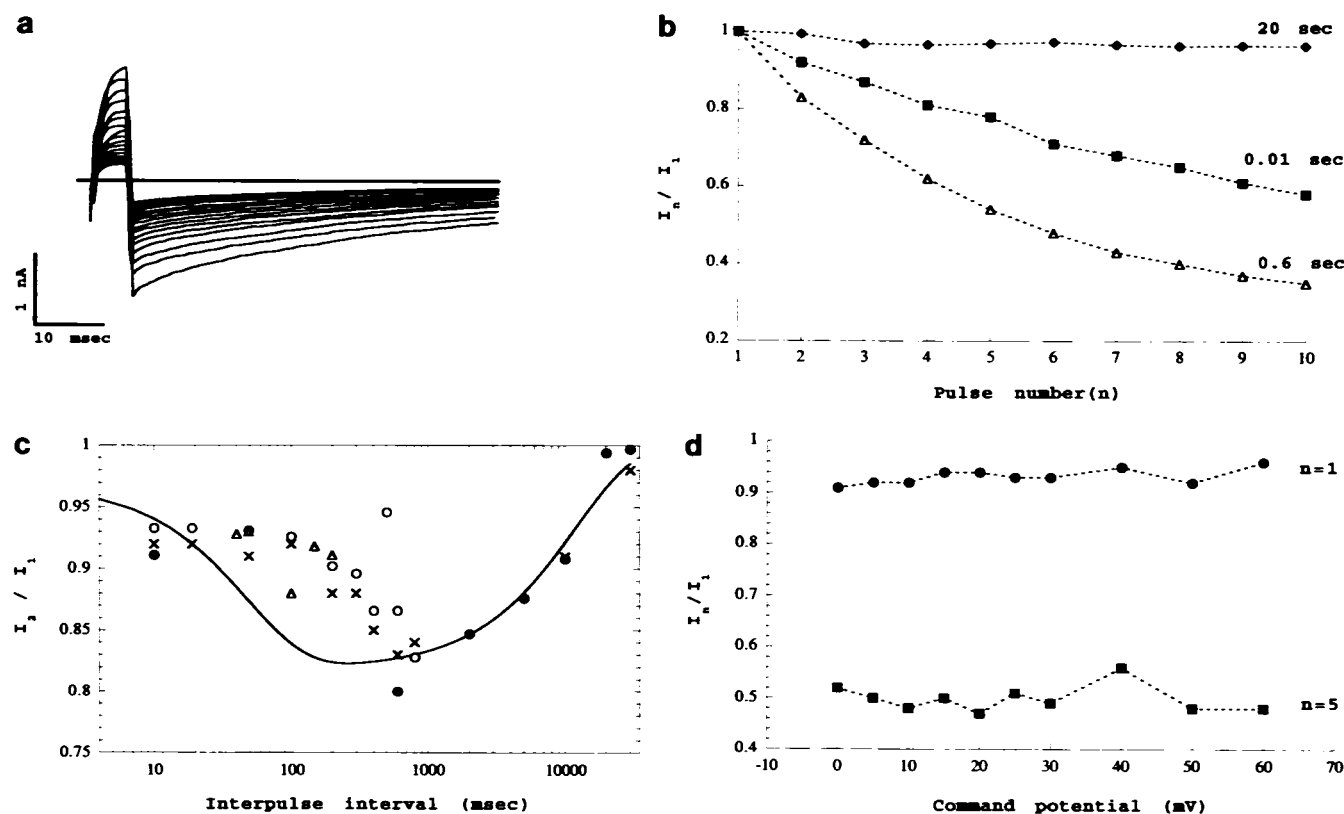

FIGURE 1 Cumulative inactivation of Kv3. (*a*) Superposition of current traces evoked by a series of 20 5 ms duration pulses to +40 mV, separated by inter-pulse intervals of 50 ms at −80 mV. (*b*) Frequency dependence of cumulative inactivation. The ratio of the peak current amplitude during each pulse, relative to that during the 1st pulse, is plotted against the pulse number (*n*) at three different interpulse intervals (next to each curve). Holding voltage −100 mV, interpulse voltage −80 mV, pulse duration 10 ms. (*c*) Biphasic recovery from inactivation. I_n/I_1 at different inter-pulse intervals from four different patches. Note the logarithmic time scale. The solid line is the prediction of the final model, which is presented and discussed later in the text. (*d*) Rate of cumulative inactivation is independent of membrane potential *during* the pulse, as measured by the ratio of I_2/I_1 and I_5/I_1 at several fully activating voltages. Interpulse interval 30 ms, pulse duration 30 ms, holding potential between pulses and pulse series is −100 mV.

channels (Scheme 1). According to this model, in cases where the deactivation transition rate is within the range of the inactivation transition rate, channels can inactivate during the deactivation (tail) phase. A branched model (Scheme 2) was suggested by Aldrich (1981) to describe inactivation of potassium channels in molluscan neurons, where cumulative inactivation is the result of fast inactivation from a closed state. According to the branched model, somewhere along the activation/deactivation pathway, channels come to a certain closed state (symbolized below as C_1) in which they face a "statistical choice": they can either proceed to the open configuration or branch directly into the inactivated state. Because the rate of recovery from the inactivated state is voltage-insensitive and very slow ($\frac{1}{10}$ s^{-1} at all voltages tested between -90 and $+80$ mV in the case of the Kv3 channel (Marom et al., 1993 and unpublished results)), inactivated channels are not available during subsequent pulses. Following is a simplified representation of the two models (voltage-dependent transitions are marked by $f(v)$, and O* represents the open state together with closely associated voltage-independent silent states):

$$C \underset{slow}{\overset{f(v)}{\rightleftharpoons}} O^* \overset{slow}{\rightleftharpoons} I$$

Scheme 1

$$C_0 \overset{f(v)}{\rightleftharpoons} C_1^* \overset{f(v)}{\rightleftharpoons} O^*$$

$$_{fast} \downarrow \quad \nearrow_{slow}$$

$$I$$
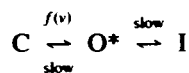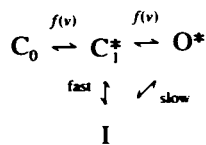
Scheme 2

Which of the two models is valid for Kv3 inactivation? The branched model predicts that, at interpulse voltages where the channel has a significant probability of occupying various closed states (represented by C_1^*) along the activation/deactivation pathway, inactivation should be faster. To test this prediction, the following pulse protocol was used (see Fig. 2). Channels were driven into the open state by a brief (5 ms) voltage pulse to a very depolarized potential ($+40$ mV); note from the amplitude of the first pulse that 5 ms is sufficient for full activation. After this activation, channels were allowed to occupy voltage-dependent closed states along the activation/deactivation pathway by holding the membrane at different hyperpolarized potentials for a short (50 ms) interpulse period, after which the membrane was stepped back to the depolarized potential. The ratio between the amplitudes of the two pulses is a measure of the rate of inactivation during the interpulse interval. As seen in Fig. 2, the amplitude of the second pulse, in fact, is larger with more hyperpolarized interpulse voltages, suggesting that inactivation cannot be accelerated by driving channels into closed states along the activation pathway. This result argues against the branched model (Scheme 2) and is consistent with the coupled model (Scheme 1), which predicts less inactivation at hyperpolarized membrane voltages, because at
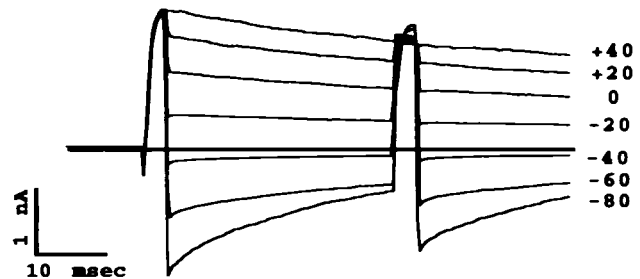

FIGURE 2   A double pulse experiment with different interpulse voltages, designed to test for voltage sensitivity of the inactivation transition (see text). Initially, the membrane is held at -100 mV for at least 1 min, after which a pair of 5 ms depolarizing pulses to $+40$ mV is delivered. The two pulses are separated by a 50 ms hyperpolarizing interpulse at the indicated voltage. The ratio of the peak current amplitude during the second pulse, relative to that during the first pulse, provides a measure for the amount of inactivation between the pulses.

these voltages the probability that the channel will close is greater than the probability that it will inactivate.

The coupled model predicts that the fraction of channels that inactivates at any given potential should be correlated with the fraction of channels that occupy the open state (O*). Fig. 3 a describes an experiment to distribute channels between, and to measure the occupancy of, three pools of channels (deactivated, open, and inactivated). This is done by a simple double pulse protocol (Fig. 3 a). Before the experiment, the patch is held for more than 1 min at -100 mV, after which the first short pulse to $+40$ mV is delivered. This pulse drives the channels to occupy the O* state. The channels are then allowed to partition between the three pools by holding the membrane at a hyperpolarized voltage (-80 mV in the example shown in Fig. 3 a) during the interpulse interval. Note that the tail current is slow and its amplitude is nonzero at the end of the interpulse period. This residual current reflects channels that are still in the O* state (see also the long tail currents in Fig. 1 a). When the second pulse is delivered, the fraction of channels that remain in the O* state (depicted as the open pool) is represented by an instantaneous change in current amplitude caused by the change in driving force. Channels that deactivated from the O* state to occupy the various closed states along the deactivation pathway (depicted as the deactivated pool) are represented by exponential activation kinetics. Finally, the difference between the amplitudes of the first and second pulses represents the inactivated pool. The results of a series of these double pulse experiments with different interpulse voltages (measured as in Fig. 3 a) are shown in Fig. 3 b. The partition between the open and deactivated pools (as well as their shapes) does not stand up quantitatively; the O* pool is over-estimated because some of the channels, which are only partially deactivated, exhibit a very rapid and unresolved rising phase (note that O* occupancy changes more than I occupancy because the interpulse interval here is very short, and inactivation requires much longer to develop fully). Nevertheless it is clear, qualitatively, that the inactivated fraction declines monotonically with more negative voltages. This result suggests that voltage-dependent transitions to the inactivated

FIGURE 3 Partitioning of channels between open, deactivated, and inactivated pools. (a) The membrane is held at −100 mV for at least 1 min, after which two pulses are delivered to the patch 20 ms apart. Channels that did not deactivate or inactivate during the interpulse interval (open pool) remain open, and they switch current flow direction instantaneously when the membrane potential is changed. Channels that deactivated during the interpulse interval (deactivated pool) show typical activation kinetics, and they peak to a level that is less than the maximum of the first pulse. The difference between the peak currents is the inactivated pool. (b) Partitioning of channels among the three pools, measured as demonstrated in a, as a function of interpulse potential. The probability of finding a channel in the inactivated pool declines monotonically with more hyperpolarized interpulse voltages. Pulse duration 5 ms, interpulse interval 50 ms. The solid line is the behavior of the inactivated pool as predicted by the final model, which is presented and discussed later in the text.
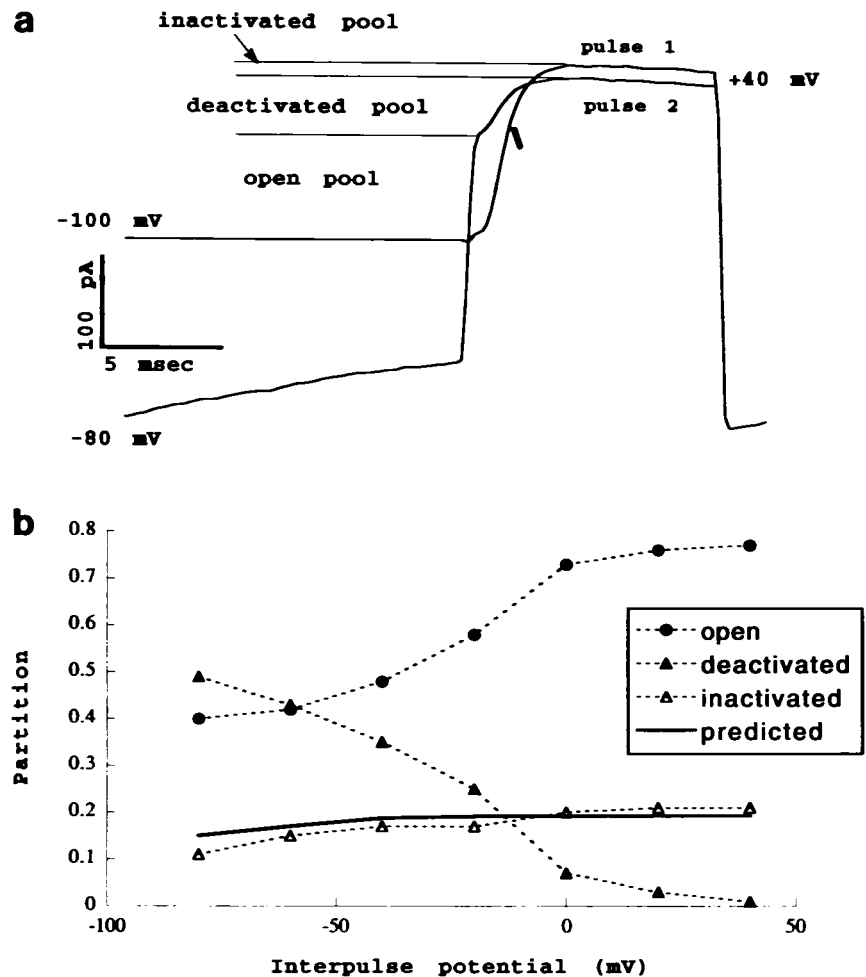
state, from closed states along the activation pathway, are not likely. Furthermore, together with the data presented in Fig. 2, these data are consistent with the coupled model (Scheme 1) for Kv3 channels. Note that in Figs. 2 and 3 b there is hardly any effect on inactivation from −40 mV and more positive, but a striking change for −60 mV and more negative. This provides a further support for the coupled model, because inactivation is independent of voltage at potentials where the channel is maximally activated (see legend to Fig. 5 for activation kinetics, and also Cahalan et al. (1985), Cukierman (1992), and Pahapill and Schlichter (1990)).

The coupled model also predicts that cumulative inactivation will depend on the rate at which channels deactivate. This prediction is tested by the experiment described in Fig. 4, in which current decrement from one pulse to the next, at different interpulse voltages, is shown. The decrement in current amplitude from one pulse to the next is much smaller at −120 mV as compared with more depolarized interpulse voltages. In other words, the rate of cumulative inactivation becomes slower as the membrane potential during the interpulse interval is hyperpolarized to more negative values, because at these potentials the open channels deactivate quickly, leaving only a small fraction to inactivate during the interpulse.

The conclusions from the experiments described above are that inactivation is a state-dependent process, coupled to the open state and intrinsically voltage-insensitive. However, apparent voltage sensitivity is conferred upon inactivation by voltage-dependent transitions before channel opening. Cumulative inactivation of the Kv3 channel is simply a different manifestation of long pulse-induced inactivation. It is induced by a unique combination of three factors: (i) a high inactivation rate/deactivation rate ratio; (ii) a lack of inherent voltage sensitivity of inactivation; and (iii) a very slow recovery from the inactivated state ($\tau = 10$ s). This mechanism for cumulative inactivation is demonstrated by the simulation in Fig. 5: a pool of activated channels is allowed to distribute between inactivated and deactivated states, as a function of time, according to the coupled model (refer to Scheme 1 above):

$$dO^*/dt = Ik_{IO} - O^*(k_{OI} + k_{OC}) + C^*k_{CO} \qquad (1)$$

$$dI/dt = O^*k_{OI} - Ik_{IO} \qquad (2)$$

$$dC^*/dt = O^*k_{OC} - C^*k_{CO} \qquad (3)$$

where k_{OI} is evaluated by fitting a single exponent to a long pulse-induced inactivation ($\frac{1}{700}$ ms^{-1}), k_{IO} is the recovery rate

FIGURE 4 Effect of interpulse voltage on the accumulation of channels in the inactivated state. Interpulse voltages are depicted to the right of each curve. Interpulse interval, 2 s; pulse duration 15 ms.
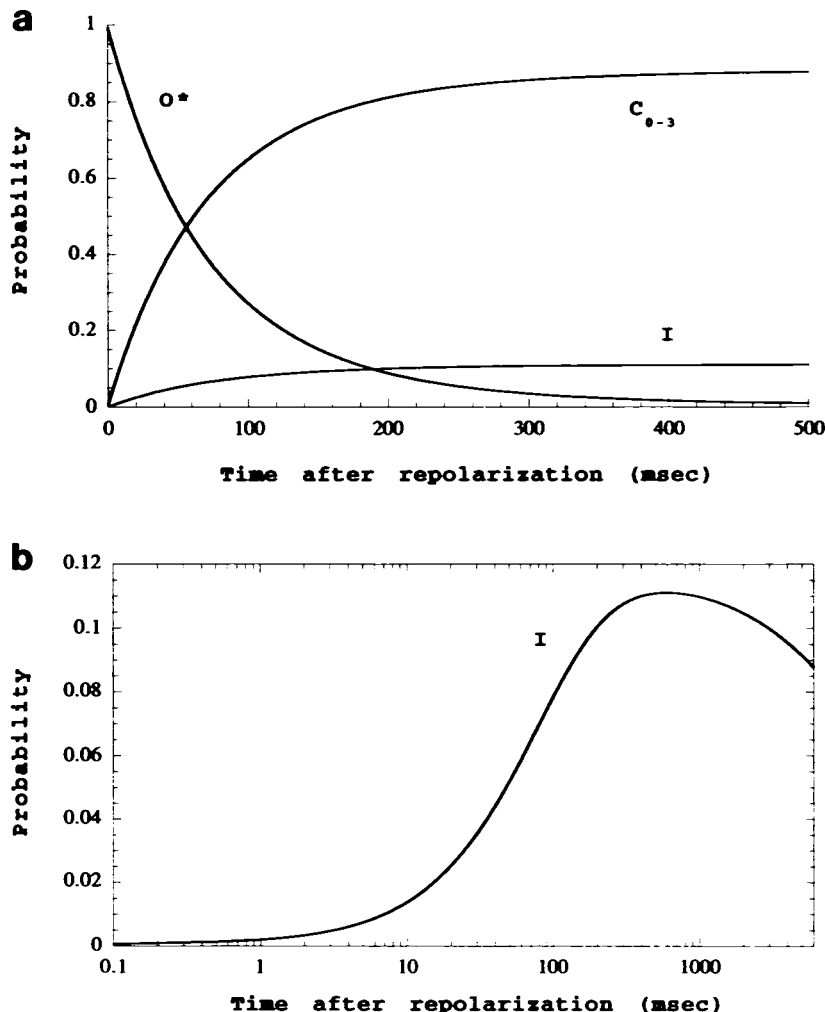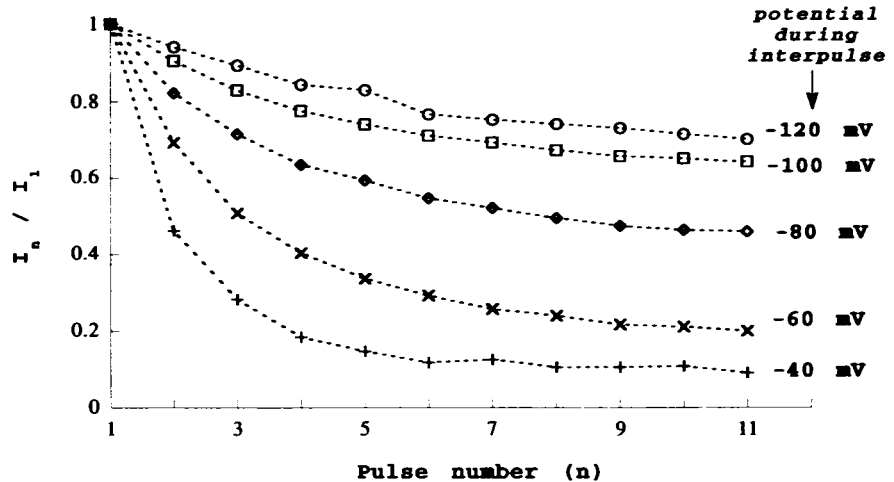

FIGURE 5 A simulation of the partitioning process as a function of interpulse duration. (a) A pool of activated channels (O*) is allowed to partition between inactivated (I) and four deactivated (C*) states during the interpulse. At $t = 0$, $O^* = 1$. Interpulse voltage is -80 mV. Note that although most of the channels occupy the deactivated states, a small but significant fraction accumulates in the inactivated state. Parameters for the model were derived as follows: Activation was fit to $Ik(t) = a(1 - \exp[-t/\tau_a])^4$ and tail currents to $Ik(t) = a\exp[-4t/\tau_a]$. Time constants for these relaxations were fit to rate equations,

$$\alpha = A(V + V_a)/(1 - \exp[-(V + V_a)/S_a]) \quad (4)$$

$$\beta = Bf\exp[-(V + V_b)/S_b] \quad (5)$$

to give a continuous function $(\alpha + \beta)$ that predicts the observed relaxation rate. A frequency factor, f, was introduced into Eq. 7 to account for voltage-insensitive flicker between active-open and active-closed states. The need for a frequency factor becomes clear whenever the rates, which are fitted from relaxations, are used for a construction of a G/G_{max} (steady-state) curve. During relaxations, f represents the probability of the channel to be in a state from which it can deactivate. However, this probability does not determine the steady-state activation curve. Equations 4 and 5 were verified by reconstructing G/G_{max} curve from $[\alpha/(\alpha + \beta/f)]^4$. $A = 0.021$, $B = 0.00166$, $f = 0.12$, $V_a = 8.3$, $V_b = 23.6$, $S_a = 9.8$, $S_b = 20.7$. In addition, the G/G_{max} curve was fitted to a boltzmann distribution, $1/(1 + e^{-(V-V_{mid})/k})$, which gave a mid-point for activation at -41.2 mV and a slope of 7.15 mV. The channel is fully activated at potentials positive to ~ -30 mV. These data are in good agreement with Cahalan et al. (1985) but slightly steeper and more negative in comparison with Lee and Deutsch (1990). (b) Biphasic occupation of the inactivated state at an expanded amplitude scale and a logarithmic time scale (see text).

from inactivation ($\frac{1}{10}$ s^{-1}, measured by use of the double pulse experiment described in Marom et al., 1993), k_{OC} and k_{CO} are the deactivation and activation rates computed from rate equations (Eqs. 4 and 5) that are described in the legend to Fig. 5. C* represents all four Hodgkin-Huxley closed states. The initial conditions for the simulation assume that all of the channels are

in the open state, and then an instantaneous hyperpolarization to -80 mV is delivered. The calculation simulates what happens to open channels during the interpulse interval at -80 mV. Fig. 5 a shows the first 500 ms: the open pool is depleted, and most channels occupy the deactivated states (depicted as C_{0-3}). However, a small but significant fraction of the channels accumulate

FIGURE 6   Single channel open (●) and closed (△) time distributions at −100 mV, measured during the interpulse interval after a depolarizing pulse. The membrane is pulsed to +40 mV (period P in *inset*) for 20 ms to activate the channel, after which the membrane is stepped back to −100 mV for the interpulse period (depicted as I in the *inset*). Distributions were constructed using 154 open events and 138 closed events during the I period. Each event was examined by eye, and durations were measured manually using a 50% threshold. τ_{open} = 6.7 ms; $\tau_{closed,1}$ = 1.2 ms (82%); $\tau_{closed,2}$ = 4.9 ms (18%). Pipet solution: 100 mM KCl, 2 CaCl$_2$, 10 HEPES. Mean inward current amplitude is 3 pA.
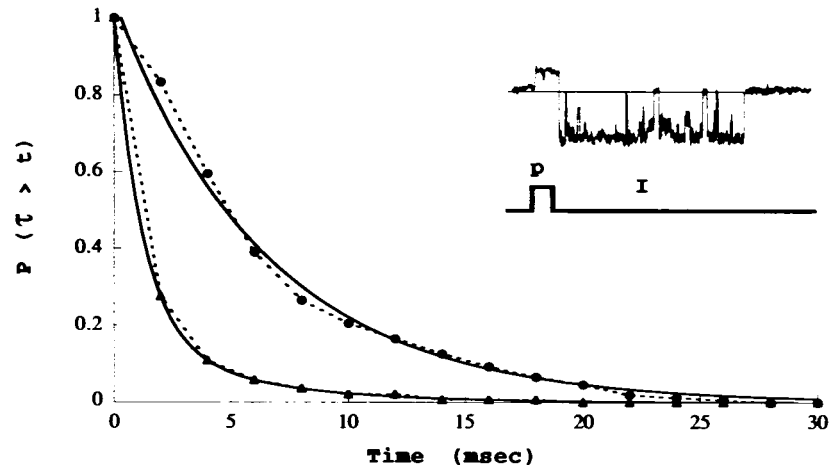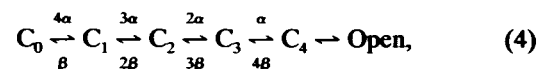

in the inactivated state (depicted as I). Fig. 5 *b* shows, at an expanded amplitude scale and a logarithmic time scale, the change in the occupancy of the inactivated state during longer time intervals at −80 mV. Note the biphasic occupation of the inactivated state, which matches the experimental observation in Fig. 1 *c*. The reason for the biphasic recovery from inactivation in this model is the following: at very short interpulse intervals, open channels do not deactivate significantly because deactivation is relatively slow and the interpulse is too short; moreover, during this short interpulse period they continue to inactivate. In this short range of interpulse intervals, the more time permitted between pulses, the more channels inactivate (rising phase of curve in Fig. 5 *b*). When the interpulse is increased further (>600 ms), recovery from inactivation is the dominant process (slow declining phase of curve in Fig. 5 *b*) because during each sojourn of the channel in the O* state it is exposed to a dominant k_{OC} (i.e., values of the rates in last C → O* step at −80 mV are 4β = 0.1 ms^{-1} and α 0.001 ms^{-1}, compared with k_{OI} = 1/700 ms^{-1}).

Although the simulation in Fig. 5 predicts much of the behavior seen in the experiment in Fig. 1 *c*, the experimental data show an unexpected feature: back extrapolation of the data seems to cross the *y* axis at a value less than unity. A single 5-ms pulse should result in less than 1% inactivation (time constant for inactivation during a pulse is 700 ms). The point at which the curve crosses the *y* axis represents a "zero" interpulse interval, and would be expected to have a value of >0.99. The fact that the actual value is ~0.92 suggests that some channels inactivate before opening. This observation does not fit a simple coupled model. However, as shown below we can, at least partially, resolve this apparent paradox by extending the model to include voltage independent transitions between open and closely associated silent states.

Inactivation is accessible from a silent state

Up to this point, the activated state has been represented as O* (see schemes above), which includes both conducting and closely associated silent states. Activated *Shaker*-related potassium channels flicker between at least one silent state and

the open state in a voltage-independent manner (Zagotta and Aldrich, 1990), spending most of their time open. It is interesting to ask which of these two states provides access into the inactivation state. This question has mechanistic implications because the measured rate of inactivation is the actual inactivation transition rate only in a case where it proceeds at identical speed from both conducting and nonconducting states. The probabilities of finding a channel in the conducting and nonconducting states, during the tail phase, can be estimated from the open and closed time distributions for a single channel at a hyperpolarized membrane potential. The single channel open and closed time distributions shown in Fig. 6 were collected at −100 mV, during the interpulse interval (I) after a depolarizing pulse (p), using the pulse protocol shown in the inset. The mean open time (6.7 ms) and mean closed time (1.2 ms) imply a probability of ~0.8 for the channel to be found in the conducting state during the tail. If inactivation is approached only from the conducting state, the actual rate of the inactivation transition is 1.25-fold faster than the value measured from the macroscopic decline during a long pulse. If, however, inactivation is approached only from the nonconducting state, the actual rate is approximately sixfold faster than the measured macroscopic rate. The single channel and macroscopic data are consistent with the following model:[1]

$$C_0 \overset{4\alpha}{\underset{\beta}{\rightleftharpoons}} C_1 \overset{3\alpha}{\underset{2\beta}{\rightleftharpoons}} C_2 \overset{2\alpha}{\underset{3\beta}{\rightleftharpoons}} C_3 \overset{\alpha}{\underset{4\beta}{\rightleftharpoons}} C_4 \rightarrow Open, \qquad (4)$$

Scheme 3

which is very similar to the activation model suggested by Zagotta and Aldrich (1990) for the *Shaker* potassium channel. Three possible simplified inactivation

---

[1] Comparison of the value of *f* from Eq. 5 (*f* = 0.12, which represents the probability of the channel to be at the state from which it can deactivate; see legend of Fig. 5), with the probability of the channel to be in the silent state (0.18, Fig. 6) suggests that the silent state is located to the left of the open state.

models are considered:

$$C_{0-3} \rightarrow C_4 \rightarrow O$$
$$\updownarrow$$
$$I$$

Scheme 4

$$C_{0-3} \rightarrow C_4 \rightleftharpoons O$$
$$\updownarrow$$
$$I$$

Scheme 5

$$C_{0-3} \rightarrow C_4 \rightarrow O$$
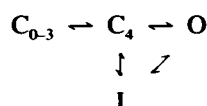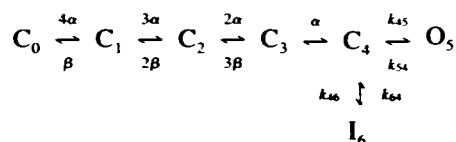$$\updownarrow \quad \diagup$$
$$I$$
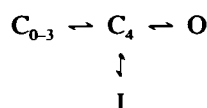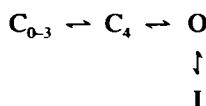
Scheme 6

All three models predict that single channel activity will be clustered, because as long as the channel escapes inactivation, it is available for subsequent pulses. However, once the channel enters the inactivated state, it will stay there for long durations because recovery from inactivation is very slow ($\tau = 10$ s). Scheme 5 does not allow a blank trace to appear after a long period of hyperpolarization; the channel *must* open before it inactivates. Scheme 5 also predicts that recovery from inactivation between pulses *must* be manifested as an opening event during the interpulse interval. An experimental paradigm, designed to test these predictions, is shown in Fig. 7 *a*. Before each experiment the channel is held at -100 mV for more than 1 min, allowing it to come to C_{0-3}. An experiment is composed of a series of 25 command sweeps: each is a 20-ms pulse to $+40$ mV followed by an interval of 200 ms at -100 mV. Data are sampled continuously throughout the experiment. Out of 15 experiments, 3 (20%) started with blank traces. Out of 12 single channel recovery events, only 7 (58%) were preceded by reopening during the interpulse interval. Furthermore, channel activity is clustered (Fig. 7 *b*). Taken together with the macroscopic current data described in Fig. 1 *c*, these results suggest that Kv3 channels need not open before they inactivate; the inactivated state is accessible from a pre-opened silent state, and Scheme 5 is not adequate. An unequivocal differentiation between Scheme 4 and Scheme 6 is not straightforward and, at present, neither can be eliminated, although for purposes of simplicity we prefer Scheme 4. Equations describing the population of each state, as a function of time, were derived for the following scheme:

$$C_0 \underset{\beta}{\overset{4\alpha}{\rightleftharpoons}} C_1 \underset{2\beta}{\overset{3\alpha}{\rightleftharpoons}} C_2 \underset{3\beta}{\overset{2\alpha}{\rightleftharpoons}} C_3 \overset{\alpha}{\rightleftharpoons} C_4 \underset{k_{54}}{\overset{k_{45}}{\rightleftharpoons}} O_5$$
$$k_{46} \updownarrow k_{64}$$
$$I_6$$

Scheme 7

a

b   Pulse number (n+1)

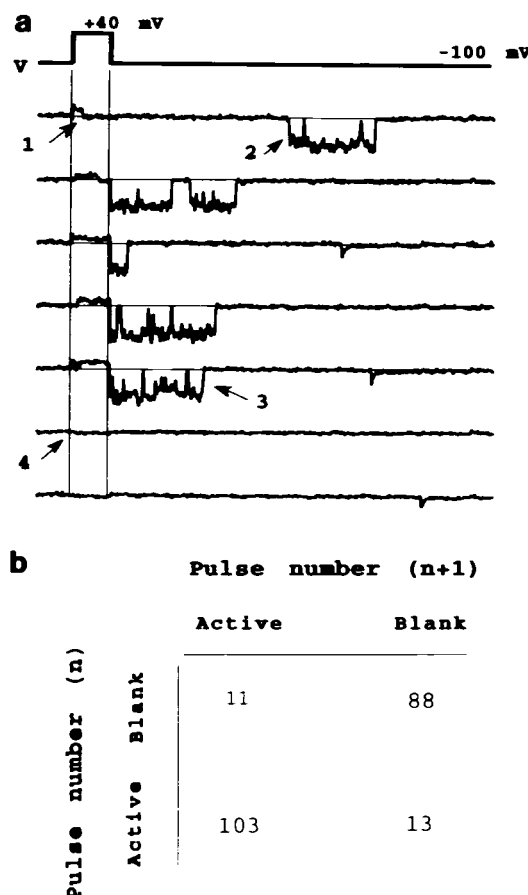|		Active	Blank
Pulse number (n)	Blank	11	88
	Active	103	13

FIGURE 7 Channel reopening upon recovery from the inactivated state during the interpulse interval. (*a*) Each sweep contains a 20-ms pulse to +40 mV, followed by an inter-pulse interval of 200 ms. Each experiment includes 25 sweeps (the figure contains seven consecutive sweeps from one representative experiment). Data are sampled continuously throughout each experiment. Arrow #1 depicts inactivation during a pulse; a reopening event during the interpulse is marked by arrow #2; channel inactivation during the interpulse interval is marked by arrow #3; and the beginning of a blank cluster is shown by arrow #4. The V-shaped current glitches seen in traces 3, 5, and 7 are caused by a discharge of head-stage capacity. (*b*) Clustering of active and blank traces, classified as described in *a*. Analysis was done by visual inspection of each individual trace, marking it as a blank if no channel opening was observed throughout the trace. Note the strong correlation between the activity at pulse number *n* and the activity at pulse number (*n* + 1).

In Fig. 8, a numerical simulation based on these differential equations is presented for a depolarization to +40 mV. It provides a reasonably accurate reconstruction of the macroscopic behavior (the *dashed line* in Fig. 8 *b* represents mean normalized current decay during long pulse inactivation ($\tau = 811$ ms, SD $= 147$, $n = 3$)). The model ($k_{46} = 1/40$ ms^{-1}) also predicts other key data described above (*solid lines* in Figs. 1 *c* and 3 *b*; see also Fig. 2 of the companion paper). These findings complicate the idealized coupled scheme (Scheme 1). However, it is possible to develop a simple expression that links the measured rate of long pulse-induced inactivation to the microscopic transition rates.

FIGURE 8   A numerical simulation of Scheme 7. Initial conditions: $C_0 = 1.0$, $V_{command} = +40$ mV. Activation and deactivation rate equations as described in Fig. 5. $k_{46} = 0.025$ ms^{-1}; $k_{64} = 0.0001$ ms^{-1}; $k_{45} = 1.2$ ms^{-1}; $k_{54} = 0.15$ ms^{-1}. (a) Expansion of the first 5 ms. (b) Longer time scale. The dashed line represents mean normalized current decay during long pulse inactivation ($\tau = 811$ ms, SD = 147, $n = 3$).
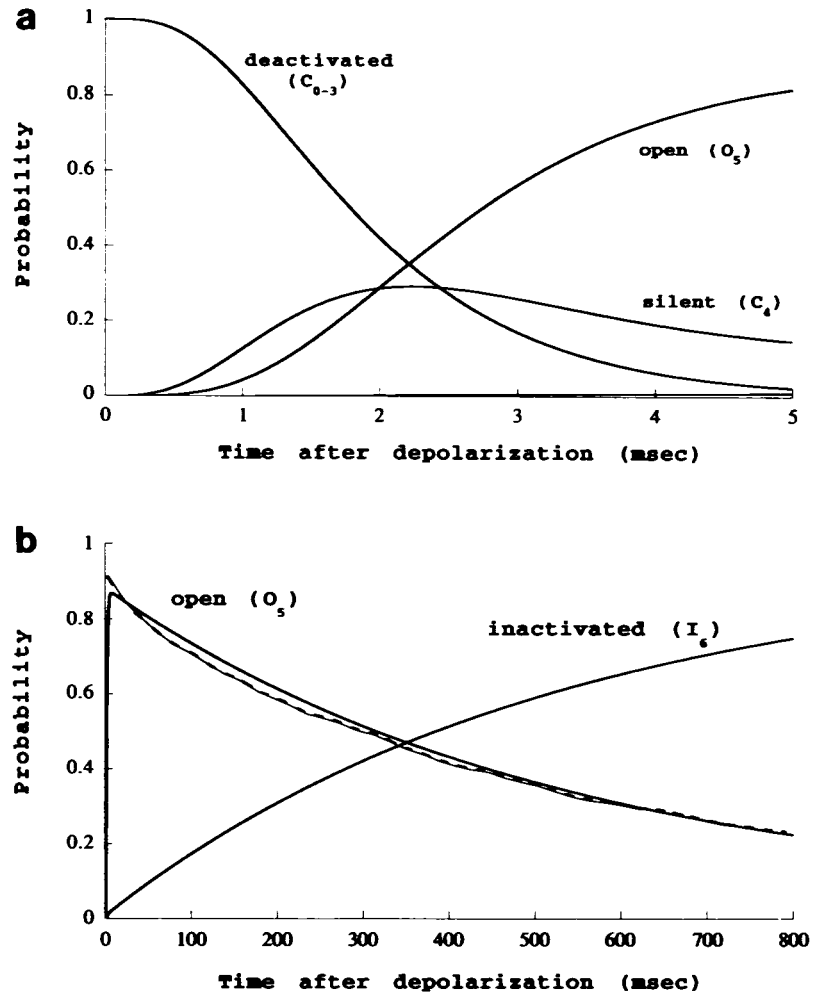
A microscopic model of inactivation

What is the relation between the rate of long pulse-induced inactivation and the transition rates $I_6 \leftrightarrow C_4 \leftrightarrow O_5$? In the case of a long depolarization to a voltage that produces full activation, (P_i being the probability of finding the channel in state i), $P_4 + P_5 + P_6 = 1$ and $\beta = 0$. Because recovery from inactivation is extremely slow, the value of k_{64} is negligible. Then,

$$dP_4/dt = k_{54}P_5 - (k_{46} + k_{45})P_4 \qquad (6)$$

$$dP_5/dt = -k_{54}P_5 + k_{45}P_4 \qquad (7)$$

$$dP_6/dt = k_{46}P_4 \qquad (8)$$

$C_4 \leftrightarrow O_5$ equilibrate very fast, so that $k_{45} P_4 = k_{54} (1 - P_6 - P_4)$ and

$$P_4 = (1 - P_6)k_{54}/(k_{45} + k_{54}) \qquad (9)$$

Substitution into Eq. 8 and integration gives

$$P_6 = 1 - \exp[-t/\tau_6] \qquad (10)$$

$$\tau_6 = (k_{45} + k_{54})/k_{46} k_{54} \qquad (11)$$

Equation 11 states simply that the rate of apparent inactivation is the $C_4 \to I_6$ transition rate times the probability of finding the channel in C_4. Substitution of these parameters with measured values ($k_{45} = 1/1.2$ ms^{-1}, $k_{54} = 1/6.7$ ms^{-1}) yields a $C_4 \to I_6$ transition rate ~one order of magnitude faster then the apparent rate of inactivation measured from the relaxation of a long pulse-induced current.

Effect of potassium and calcium on slow inactivation: a working hypothesis

External potassium has been reported to have three apparently unrelated effects on the current carried by Kv3 channels: (i) the rate of inactivation in the lymphocyte potassium channel (Grissmer and Cahalan, 1989), as well as in several other delayed rectifier channels (DeCoursey, 1990), is sensitive to the concentration of external potassium; (ii) the deactivation rate is slowed by increasing external potassium concentration (Cahalan et al., 1985); and (iii) macroscopic currents, carried by Kv3 channels, are reduced when external potassium is decreased (Pardo et al., 1992). In Fig. 9 a, the effect of varying external potassium concentration on the rate

FIGURE 9 Effects of external potassium and external calcium on the rate of long-pulse induced inactivation. (a) Current was evoked by a depolarization to +40 mV for 800 ms. Mean (n = 3, SD bars) normalized relaxations in different ionic concentrations as indicated. Sodium ions were used to balance the osmolarity. (b) Expected vs observed long-pulse induced inactivation time constants. Hollow symbols denote observed SD. Each point is the average of three time constants. The time constant expected from the model (■) calculated from Eq. 12 with the parameters mentioned in the text.
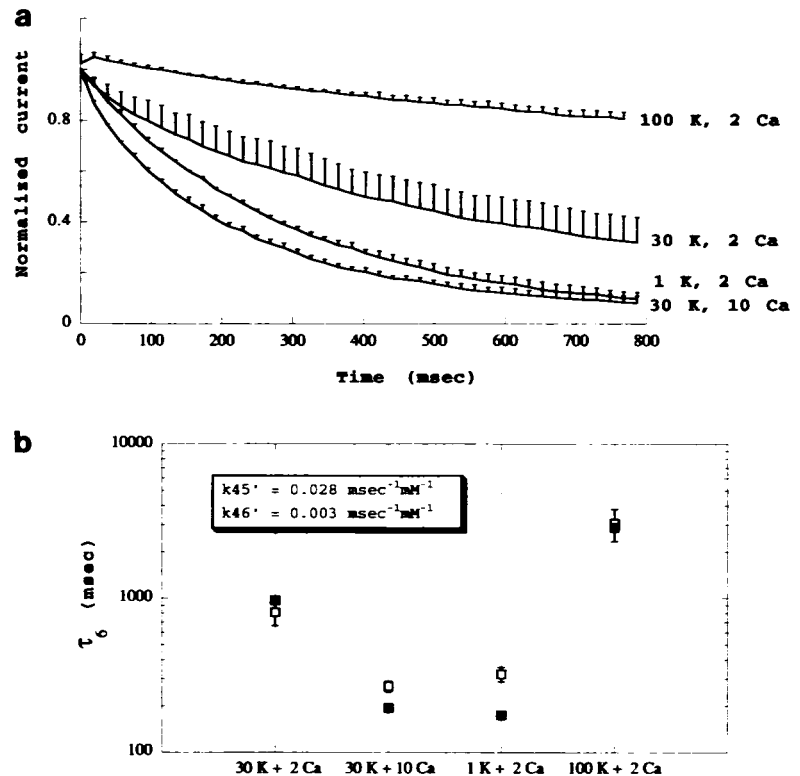
of long pulse-induced inactivation is demonstrated. Increasing external potassium concentration from 1 to 100 mM results in a marked slowing of inactivation. The microscopic model developed in this study can account for these effects of potassium, if potassium is required for the $C_4 \rightarrow O_5$ transition. This provides a unifying explanation for the three observed effects of external potassium on the channel. Furthermore, as shown in Fig. 9 a, increasing external calcium concentration from 2 to 10 mM markedly enhances the rate of macroscopic inactivation. Grissmer and Cahalan (1989) have shown that calcium and potassium ions compete for binding to the external mouth of the lymphocyte potassium channel. These observations can be explained by an involvement of calcium in the $C_4 \rightarrow I_6$ transition. Use of Eq. 12 to get a rough estimate of the binding rates of potassium and calcium ions to their external site (s), yields a reasonably good reconstruction of the data:

$$\tau_6 = (k'_{45}[K_0] + k_{54})/k'_{46}[Ca_0]k_{54} \qquad (12)$$

The time course of relaxations, in different potassium and calcium concentrations (Fig. 9 a, b), yield k'_{45} and k'_{46} values of 0.028 and 0.0034 ms^{-1} mM^{-1}, respectively. The calculated K_d for external calcium binding is ~30 μM, whereas the K_d for potassium binding is ~5.4 mM.

DISCUSSION

We have examined mechanisms of inactivation of Kv3 potassium channels. The biophysical data are consistent with a model in which channels do not need to open before they inactivate. Inactivation branches rapidly from a silent state

that is closely associated with, and positioned just before, the open state. During a long depolarizing pulse, channels flicker between the open and silent states, and in each sojourn in the silent state the channels have a chance to inactivate. Inactivation from the silent state is severalfold faster then the current decay rate within a long pulse. This is because the low probability of the channel to be in the silent state at depolarized voltages slows the apparent inactivation rate. The mechanism of inactivation is similar to a mechanism suggested by DeCoursey (1990) for the alveolar epithelial potassium channel, where inactivation proceeds during the tail phase. We have described previously (Marom et al., 1993) an acceleration of cumulative inactivation rate, accompanied by a parallel slowing of deactivation kinetics, upon going from the cell-attached to the -detached patch recording mode. These observations, together with the results reported in the present study, suggest that a modulation of deactivation rate contributes to the faster rate of cumulative inactivation when the patch is detached from the cell.

Inactivation in the Kv3 potassium channel has features that are interesting from the molecular-biophysical point of view. A working hypothesis for the involvement of potassium and calcium ions in the process of gating is presented, where potassium is required for a transition that leads into the open state and calcium is required for a transition that leads into the inactivated state. This hypothesis is supported by Pardo et al. (1992) who reported no effect of external potassium on mean open time for the RCK4 channel. Other support for this model comes from Lopez-Barneo et al. (1993), who observed an augmentation of *Shaker* macroscopic current amplitude in high external potassium caused by an increase in channel

availability rather than by drastic changes in channel conductance. Grissmer and Cahalan (1989) found that the effect of potassium on the lymphocyte channel follows a Hill function with a slope of 1.1, suggesting that the potassium effect is mediated by a simple bimolecular binding reaction. Appealing as it might be, our model for a potassium effect on the Kv3 channel is rather simplified. For example, Pardo et al. (1992) were not able to eliminate completely the Kv3 current during perfusion with potassium-free external solutions. Further complication comes from the observation by Cahalan et al. (1985) of an increase in the lymphocyte potassium channel unitary conductance in high external potassium. As in the case of the potassium effect, the suggested mechanism for the action of calcium might be incomplete, because replacing calcium with magnesium does not eliminate inactivation (data not shown; also see Grissmer and Cahalan, 1989). Despite the above reservations, the fit of our data by Eq. 12 is surprisingly good, suggesting that these mechanisms deserve closer examination at the single channel level.

Although the notion of ions serving as "gating particles" is not new (e.g., Grissmer and Cahalan, 1989; Armstrong and Natteson, 1986), the Kv3 channel offers a basis for structure-function studies of the well documented involvement of potassium and calcium ions in gating of delayed rectifier channels. We already know that a particular amino acid residue, His-401, is significant for potassium binding and inactivation in Kv3 (Busch et al., 1991; Pardo et al., 1992) and *Shaker* (Lopez-Barneo et al., 1993) channels. It remains to be determined what other residues are important for binding of potassium ions to the external mouth of the channel, or whether calcium competes with potassium for the same site in the Kv3 channel.

There are several limitations to the preferred final model (Scheme 7). The model does not explain another faster (but less significant) inactivation process that seems to occur within the first few milliseconds (e.g., measured versus expected traces in Fig. 8 b). It also does not explain the small gap between expected and measured pre-opened inactivation (Fig. 1 c). It does not consider a second silent state that is coupled to the open state as suggested by the bi-exponential fit to the closed time distribution (Fig. 6). It is probably possible to fine-tune the model (at the price of increased complexity) by adding more transitions to inactivated state from other states along the activation pathway. However, the preferred model captures the main features of inactivation in the cloned Kv3 channel (including cumulative inactivation) and provides a simple starting point for macroscopic simulation studies (companion manuscript) and structure-function analysis.

Inactivation of the Kv3 channel has interesting physiological consequences. The presence of cumulative inactivation in Kv3 channels of excitable membranes will make no significant contribution to the rate and duration of sporadic action potentials, because a single action potential is too short to induce inactivation. However, the effect becomes very significant when a train of action potentials occurs. Under these conditions, the availability of Kv3 potassium channels is de-

creased as a function of firing frequency. Moreover, because recovery from inactivation is extremely slow, more than 30 s is required for the channels to completely "forget" the effect of previous stimulations. Rahamimoff et al. (1992) reported similar behavior of a synaptosomal bursting potassium channel, and termed this phenomenon "statistical memory." They speculate that cumulative inactivation plays a part in frequency modulation of transmitter release. In a companion paper (Marom and Abbott, 1994) we develop a macroscopic model that describes state-dependent inactivation in terms of Hodgkin and Huxley formalism. We then use this model to study the effects of Kv3 inactivation on the activity of a model neuron.

REFERENCES

Aldrich, R. W. 1981. Inactivation of voltage-gated delayed potassium current in molluscan neurons. *Biophys. J.* 36:519–532.

Armstrong, C. M., and D. R. Matteson. 1986. The role of calcium ions in the closing of K channels. *J. Gen. Physiol.* 87:817–832.

Busch, A. E., R. S. Hurst, R. A. North, J. P. Adelman, and M. P. Kavanaugh. 1991. Current inactivation involves a histidine residue in the pore of the rat lymphocyte potassium channel RGK5. *Biochem. Biophys. Res. Commun.* 179:1384–1390.

Cahalan, M. D., K. G. Chandy, T. E. DeCoursey, and S. Gupta. 1985. A voltage-gated potassium channel in human T lymphocytes. *J. Physiol.* 358:197–237.

Cukierman, S. 1992. Characterization of K currents in rat malignant lymphocytes (Nb2 cells). *J. Membr. Biol.* 126:147–157.

DeCoursey, T. E. 1990. State-dependent inactivation of K currents in rat type II alveolar epithelial cells. *J. Gen. Physiol.* 95:617–646.

Douglass, J., P. B. Osborn, Y. C. Cai, M. Wilkinson, M. J. Christie, and J. P. Adelman. 1990. Characterization and functional expression of a rat genomic DNA clone encoding a lymphocyte potassium channel. *J. Immunol.* 144:4841–4850.

Grissmer, S., and M. Cahalan. 1989. Divalent ion trapping inside potassium channels of human T lymphocytes. *Biophys. J.* 55:203–206.

Grissmer, S., B. Dethlefts, J. J. Wasmuth, A. L. Goldin, G. A. Gutman, M. D. Cahalan, and K. G. Chandy. 1990. Expression and chromosomal localization of a lymphocyte K channel gene. *Proc. Natl. Acad. Sci. USA.* 87:9411–9415.

Hille, B. 1992. Ion Channels of Excitable Membranes. Sinauer Associates, Sunderland, MA.

Honore, E., B. Attali, G. Romey, F. Lesage, J. Barhanin, and M. Lazdunsky. 1992. Different types of K channel current are generated by different levels of single mRNA. *EMBO J.* 11:7:2465–2471.

Hoshi, T., W. N. Zagotta, and R. W. Aldrich. 1991. Two types of inactivation: effects of alterations in carboxy-terminal region. *Neuron.* 7: 547–556.

Koren, G., E. R. Liman, D. E. Logothetis, B. Nadal-Ginard, and P. Hess. 1990. Gating mechanism of a cloned potassium channel expressed in frog oocytes and mammalian cells. *Neuron.* 2:39–51.

Lee, S. C., and C. Deutsch. 1990. Temperature dependence of K-channel properties in human T lymphocytes. *Biophys. J.* 57:49–62.

Lopez-Barneo, J., T. Hoshi, S. H. Heinemann, and R. W. Aldrich. 1993. Effects of external cations and mutations in the pore region on C-type inactivation of *Shaker* potassium channels. *Receptors and Channels.* 1:61–71.

Marom, S., S. A. N. Goldstein, J. Kupper, and I. B. Levitan. 1993. Mechanism and modulation of inactivation of the Kv3 potassium channel. *Receptors and Channels.* 1:81–88.

Marom, S., and L. F. Abbott. 1994. Modeling state dependent inactivation of membrane currents. *Biophys. J.* 67:515–520.

Pahapill, P. A., and L. C. Schlichter. 1990. Modulation of potassium channels in human T-lymphocytes: effects of temperature. *J. Physiol.* 422: 102–126.

Pardo, L. A., S. H. Heinemann, H. Terlau, U. Ludwig, C. Lorra, and W. Stühmer. 1992. Extracellular K specifically modulates a rat brain K channel. *Proc. Natl. Acad. Sci. USA.* 89:2466–2470.

Rahamimoff, R., J. Edry-Schiller, and S. Ginsburg. 1992. A long closed state of the synaptosomal bursting potassium channel conferred a statistical memory. *J. Neurophysiol.* 68:2260–2263.

Stühmer, W., J. P. Ruppersberg, K. Schröter, B. Sakmann, M. Stocker, K. Giese, A. Perschke, A. Baumann, and O. Pongs. 1989. Molecular basis of functional diversity of voltage-gated potassium channels in mammalian brain. *EMBO J.* 8:3235–3244.

Swanson, R., J. Marshall, J. S. Smith, J. B. Williams, M. B. Boyle, K. Folander, C. J. Luneau, J. Antanavage, C. Oliva, S. A. Buhrow, C. Bennett, R. B. Stein, and L. K. Kaczmarek. 1990. Cloning and expression of cDNA and genomic clones encoding three delayed rectifier potassium channels in rat brain. *Neuron.* 4:929–939.

Zagotta, W. N., and R. W. Aldrich. 1990. Voltage-dependent gating of Shaker A type potassium channels in *Drosophila* muscle. *J. Gen. Physiol.* 95:29–60.